Available online at www.sciencedirect.com
SCIENCE DIRECT
C. R. Physique 6 (2005) 1081–1088
COMPTES RENDUS PHYSIQUE
http://france.elsevier.com/direct/COMREN/

MCAO for very large telescopes/OAMC pour les très grands télescopes

Multi-Conjugate Adaptive Optics for ELTs: constraints and limitations

Roberto Ragazzoni, Brice Le Roux *, Carmelo Arcidiacono

Osservatorio astrofisico di Arcetri, Largo Fermi, 5, 50125 Firenze, Italy

Abstract

We present how enlarging the size of a telescope from the current 10 meter telescope to the future 100 meter Extremely Large Telescopes increases the complexity of a classical or multiconjugate adaptive optics instrument. We point out elements or parameters of the system for which it is critical to propose new ideas as solutions and we study the effect of the increase of the diameter on the point spread function of an MCAO and a Ground Layer AO system. ***To cite this article: R. Ragazzoni et al., C. R. Physique 6 (2005).***

Résumé

Optique adaptative multi-conjuguée pour les télescopes extrêmement grands (ELTs) : contraintes et limitations. Nous discutons l'effet sur la complexité des systèmes d'optique adaptative, classique ou multi-conjuguée, du passage des télescopes actuels, de 10 mètres de diamètre, aux futurs ELTs pouvant atteindre 100 mètres de diamètre. Nous mettons en évidence certains élements et paramètres cruciaux qui imposent d'avoir recours à de nouveaux concepts et empêchent une simple mise à l'échelle des systèmes existants. Nous étudions finalement l'effet de l'augmentation de diamètre du télescope sur la densité spectrale de puissance du système, en distinguant les cas de l'optique adaptative « couche au sol » et multiconjuguée. ***Pour citer cet article : R. Ragazzoni et al., C. R. Physique 6 (2005).***

Keywords: Multiconjugate adaptive optics; Extremely Large Telescopes

Mots-clés : Optique adaptative multi-conjuguée ; Télescopes extrêmement grands

1. Introduction

Adaptive Optics (AO) allows today's 10-m class telescopes to obtain diffraction limited astronomical images. From the first systems [1] to more recent ones [2,3], the size of the telescope has enlarged, the complexity of the AO system has increased and its structure itself has evolved. The new challenges of making diffraction limited images with Extremely Large Telescopes (ELT), up to 100 m in diameter, make even more clear the necessity to improve and change our way of designing AO systems. On the other hand, Multiconjugate AO (MCAO) was proposed a few decades ago [4–6] to deal with the fundamental problem

* Corresponding author.
E-mail addresses: ragazzoni@arcetri.astro.it (R. Ragazzoni), leroux@arcetri.astro.it (B. Le Roux), carmelo@arcetri.astro.it (C. Arcidiacono).

1631-0705/$ – see front matter
doi:10.1016/j.crhy.2005.12.007

of anisoplanatism in classical AO. Based on the use of several Guide Stars (GS) to sense the turbulent volume and several Deformable Mirrors (DM) conjugated to different altitudes to correct it, this concept obviously increases AO complexity. The first working MCAO systems should be completed in the next few years [9–12,7,8]. Noting that the AO system of an ELT should be an MCAO in order to have access to a reasonable imaging field of view, one should understand that the complexity is increasing in a huge way.

A simple scaling of the major elements of the system gives a first qualitative impression. Increasing the size of the telescope by a factor 10 means roughly increasing by a factor 100 the number of sub-apertures on the wave-front sensor and the number of actuators on the mirror. Passing from a near infra-red system to a visible system also means increasing by a factor 10 the number of sub-apertures and actuators. By increasing finally the number of reference stars by a factor 10, one can obtain that the size of an interaction matrix of such a system increases from $N \times N$ to roughly $N \cdot 10^4 \times N \cdot 10^4$, which would mean an increase of the computational power of the order of $10^8 \ldots$.

This kind of argument, even if it allows us to understand qualitatively the increase of complexity, is rarely quantitatively relevant. Such challenges require generally new solutions [13] to be developed.

The idea that an AO system designed for an ELT would not look like that designed for a 10-m class telescope is, first of all, based on the fact that the physical conditions and regime in which such a system would work, are fundamentally different.

Even if a 10-m class MCAO system was entirely scaled for a 100-m class telescope, there is one major element that always remains unscalable: the atmospheric turbulence. Obviously, neither layer altitude nor atmospheric parameters are scaled. Therefore, the telescope diameter becomes huge with respect to the Fried parameter r_0, which means that light is strongly spread around, and the halo in the Point Spread Function (PSF) becomes very large compared to the diffraction limit. This will be detailed in Section 2.4.

Moreover, the altitude of the layers remains identical and the footprint overlap at the turbulence altitude becomes much larger than previously. This will be explained in more details in Section 2.3.

The turbulence outer scale L_0 does not change either, and the size of the telescope becomes of the order of L_0 or larger. This means that the energy contained in the low spatial frequencies becomes much smaller. We will detail this in Section 2.2.

Finally, for systems considering laser guide stars [14], the working regime of the guide star is also quite different. As an example, as the altitude of the sodium layer H_{Na} remains identical, as well as its thickness T_{Na}, the elongation of the beacon increases with D

$$D \times T_{\mathrm{Na}}/H_{\mathrm{Na}}^2 \gg \lambda/r_0 \tag{1}$$

and

$$D/H_{\mathrm{Na}} \gg FoV \tag{2}$$

As the telescope diameter increases, the elongation of the Laser Guide Star (LGS) as seen from the edge of the telescope increases and becomes huge for a 100 m scale telescope (several arcsec). Moreover, given the same focal ratio, the focus of the LGS is much more distant from the focal plane.

Rayleigh LGS becomes very, very difficult and non conventional LGS wavefront sensings (PIGS [20], SPLASH [21], others) might be investigated.

We will explore here the different elements and parameters of an MCAO system and expose the consequence of a simple scaling from 10 to 100 meters on mirror technology and the effect of the outer-scale. We will investigate the effects on the PSF.

2. Scaling adaptive optics, from 10 to 100 meters

2.1. Deformable mirrors

The first limiting parameter concerning a deformable mirror for an ELT is obviously the huge number of actuators. The feasibility of AO for ELT is thus strongly dependent on technological capabilities. Making huge mirrors with a huge number of actuators, even if challenging, is mandatory.

Several ways to realize such a display are today investigated in parallel studies. The first uses micromachining techniques, such as Micro Electro-Mechanical Systems [18] (MEMS). This technological solution would allow us to obtain the most compact and practical mirrors, but the actual micro-actuators, unfortunately, give a too small stroke to allow a proper correction.

A second solution for mirrors for ELTs is explored in the realization of the adaptive secondary mirror of the Large Binocular Telescope [17]. Fig. 1 illustrates the complexity of such a system: the tip-tilt correction of low frequency is applied, moving the exapod mount, while the 672 electromagnetic actuators control the correction to be applied to the thin shell. However, this kind of mirror, as it has been realized for LBT, gives a pitch (interactuator distance) that can be too large to be used in several tertiary or quaternary designs. New approaches might be investigated to obtain mirrors with a smaller pitch or, for example,

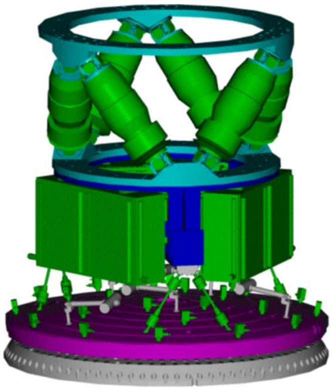

Fig. 1. A sketch of the deformable secondary mirror of the LBT.

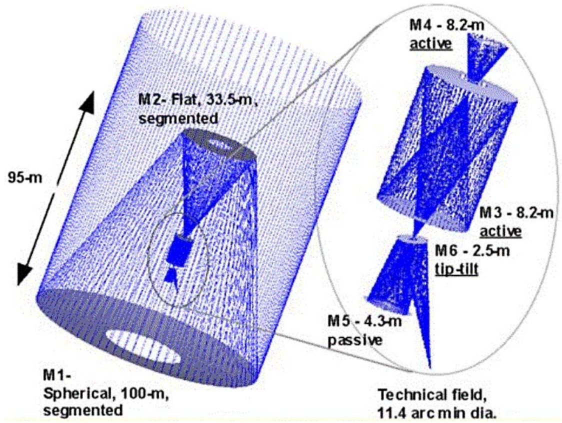

Fig. 2. A design for the OWL telescope, including 6 DMs.

to create deformable primary mirrors, even if this last solution would certainly be difficult to realize for nontechnical reasons (cost, industrial readiness for big quantities).

The design of the Overwhelmingly Large telescope [19] [OWL] is shown in Fig. 2, where it can be seen that the size of mirrors M_5 and M_6 are 4.3 and 2.5 meters, respectively. It is thus already possible to activate mirrors M_5 and M_6 of the OWL, for instance in the near infrared band. It is also possible to realize mirrors in a modular way, such as the segmented M_1 and M_2, each segment being then of an acceptable size to make a deformable mirror.

2.2. *Effect of the outer-scale*

Current atmospheric measurements present outer-scales (L_0) values between 20–100 m, related to a Von Karman power spectrum for the spatial distribution of the optical turbulence. For an ELT, the diameter of the telescope becomes comparable, or even larger than this outer scales value: this implies that for ELT the Zernike tilt due to the atmospheric turbulence becomes sensitively small compared to the overall tilt experienced by 10 m class telescopes. The statistics of the turbulence seen at the ELTs scale is no longer Kolmogorov. In fact, if the ratio D/L_0 increases up to infinity, the distribution of energy onto the spatial frequencies is more and more flat, and on size larger than L_0 there is the same amount of energy in the low and high frequencies [15]. A trivial effect is on the DM stroke needs, because tip-tilt becomes smaller and smaller, going in the direction favorable to the design of deformable mirrors. One could actually consider using the same mirror to correct the tip-tilt and the larger order modes, without any dedicated tip-tilt mirror. Of course, the tilt due to wind buffeting or a tracking error becomes predominant, but this one is full sky isoplanatic and it has typical temporal frequencies much smaller than the optical one.

2.3. *Large overlap of pupils and field of view*

If a 8 m class MCAO system is entirely scaled to a 100 m class telescope, there is one major element that always remains unchanged: atmospheric turbulence. Obviously, neither layer altitudes nor atmospheric parameters scales with pupil size. This implies a first immediate consequence on the footprint overlap of the telescope along two directions at different altitudes (Fig. 3). In the 8 m-telescope case, the footprints are totally separated and turbulence is uncorrelated from one footprint to the other. In the 100 m-telescope case, the footprints are much still overlapping and the correlation is high. If we denote FoV the field of view, $H_{\text{turbulence}}$ the mean altitude of the layers, the maximum displacement of the pupil on the whole field of view is $H_{\text{turbulence}}\tan(FoV)$ where tan() stands for the tangent function. In the approximation of small angles, we obtain $H_{\text{turbulence}}\tan(FoV) \approx FoV\,H_{\text{turbulence}}$ and:

$$FoV\,H_{\text{turbulence}} \ll D \tag{3}$$

This is particularly true for the lower modes of correction that, hence, will be essentially identical for various points over the Field of View. The immediate consequence is that the turbulence contained in the higher layers cannot be seen nor corrected by a single mirror on the pupil plane in the case of the 8 m class telescope, while in the 100 m telescope case, the higher layers are partially sensed and corrected by the AO system. This implies that it might be easier to increase the anisoplanetic field after the MCAO system for a 100 m class telescopes than for a 10 m class telescope.

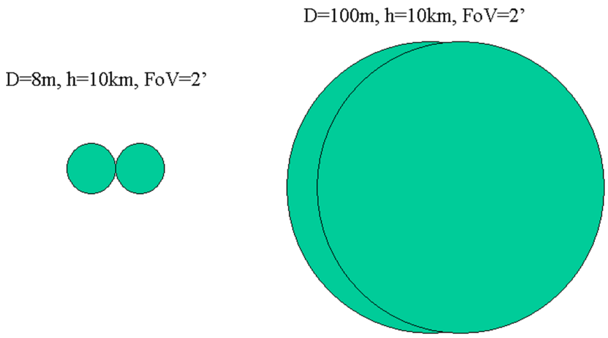

Fig. 3. Difference of separation of the footprints at high altitude for a 8 m and 100 m telescope.

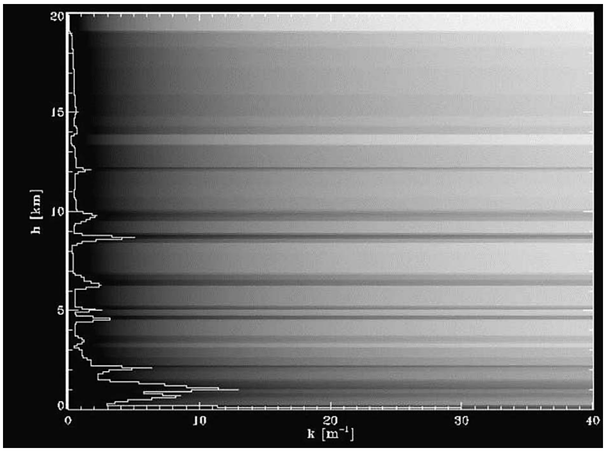

Fig. 4. Illustration of the atmospheric turbulence, presented on two axis, the spatial frequency and the altitude.

Moreover, the thickness of the slab of turbulence being efficiently compensated by a system depends upon the FoV where the correction has to be achieved and the spatial sampling on the pupil. A system correcting on a larger FoV corrects smaller slabs of turbulence.

It is possible to make a bi-dimensional representation of the atmospheric turbulence by plotting in grey-scale the energy of the turbulence for each spatial frequency (x axis) and the atmospheric altitude (y axis). An example of this representation is given in Fig. 4. As the Kolmogorov statistics lower spatial frequencies contain more energy, at the same altitude, the representation is darker on the left (low order modes) than on the right (high order modes). Furthermore, it is darker at the altitude at which the C_n^2 is higher.

With this representation, we illustrate on Fig. 5 how the correction degrades far away from the DM as a smoothing effect. It is known that a mirror can correct only the low spatial frequencies of a layer located at a distance δh, up to the cut off frequency $f_c = 1/(FoV\delta h)$. This is known as the generalized fitting effect [16]. We present on Fig. 5-left the mirror correction corresponding to the turbulence located at the same altitude. The $3d$ wavefront contains high spatial frequencies. On Fig. 5-right, we present the mirror correction corresponding to the turbulence located at a different altitude. The $3d$ wavefront contains only low spatial frequencies.

In the same way, we present on Fig. 6 the behaviour of the smoothing effect of the mirror correction for different FoV. We present on Fig. 6-left the mirror correction for a small FoV. The $3d$ wavefront contains high spatial frequencies. On Fig. 6-right, we present the mirror correction corresponding to a larger FoV. The $3d$ wavefront contains only low spatial frequencies.

2.4. Scaling the PSF, ground layer and multiconjugate AO

For a 100-m scale telescope, D/r_0 is extremely large and the size of the halo (λ/r_0), compared to the core (λ/D), becomes huge, so that the surface brightness of the halo is very faint.

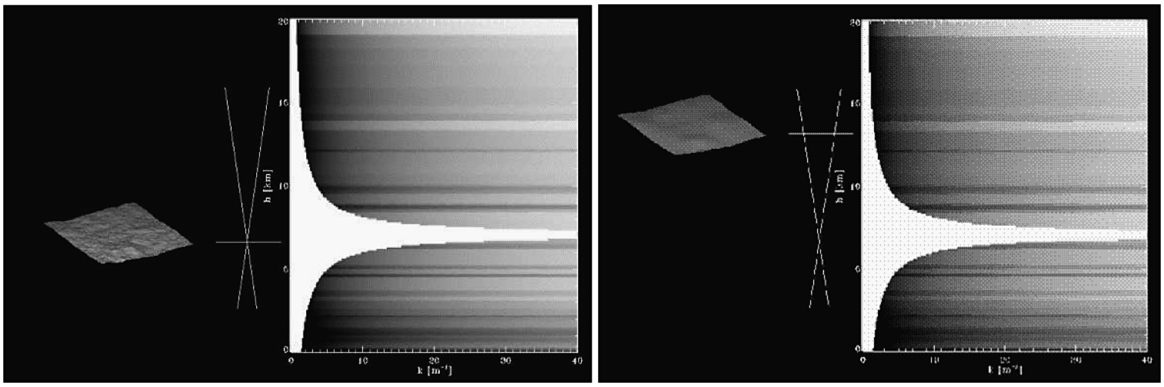

Fig. 5. Illustrations, in the frequency-altitude plane, of the correction away from the DM, at a given FoV. Far away from the mirror, only the lower order modes are corrected, as a smooth effect.

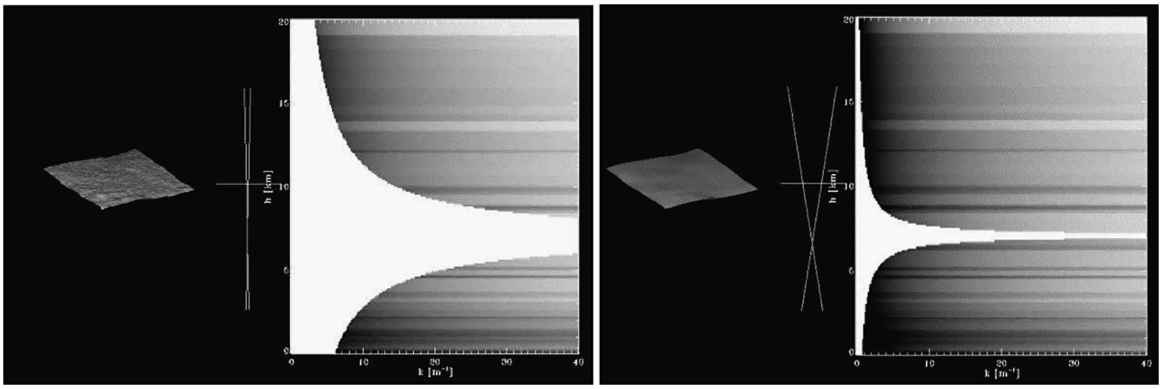

Fig. 6. Illustrations, in the frequency-altitude plane, of the correction for different FoV, at a given altitude.

This would suggest that an AO system for an ELT can 'easily' reach the Planet Finding regime, thanks to the high contrast peak/halo. In fact, the pertinent parameter for the Planet Finding regime is the visibility of the planet V_{planet}, this being the intensity ratio between the core of the planet image and the halo corresponding to the star image, which can be expressed:

$$V = \frac{I}{(1-S)/(D/r_0)^2} \tag{4}$$

where I is the intensity of the planet and S is the Strehl Ratio achieved by the system.

We note with this formula that to obtain the same visibility V with a 8 m telescope compared with the visibility obtained on a 100 m telescope at $S_{100m} = 30\%$ of Strehl, you have to achieve a Strehl S_{8m} such that:

$$\frac{100^2}{1-S_{100m}} = \frac{8^2}{1-S_{8m}} \tag{5}$$

this gives finally $S_{100m} = 0.3$, $S_{8m} = 0.995$.

A Strehl ratio of 30% for $D = 100$ m is then equivalent to a Strehl ratio of 99.5% for $D = 8$ m in terms of planet visibility, which confirms that an AO system for an ELT can reach the Planet Finding regime much more easily than for a 8 m class telescope. We have plotted in Fig. 7 the ratio $\frac{1}{(1-S)/(D/r_0)^2}$ for $D = 100$ m and 8 m and for $r_0 = 0.2$ m as a function of S in order to illustrate this phenomena.

For ELTs, Ground Layer Adaptive Optics (GLAO) and MCAO are both possible to extend the isoplanatic path. However, the PSF of both systems are quite different.

The behavior of the adaptive correction is different, and, for a diameter size larger than the turbulence outer-scale (L_0), it starts to play a role also without any correction, in open loop conditions. On these large sizes the overlap of the pupils in the different directions included in the field of view is much larger. We define the limit altitude: $h_{\text{lim}} = D/FoV$, where D is the

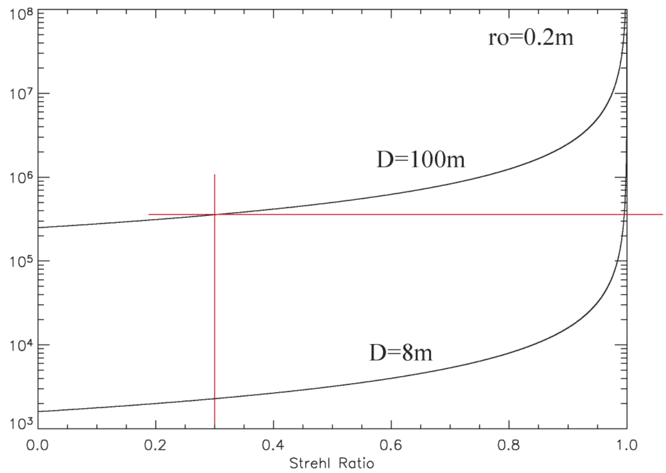

Fig. 7. Ratio between the intensity in the core of an exoplanet image and the halo corresponding to the star image, for a 100 m and 8 m telescope.

diameter of the telescope and *FoV* is the Field of view. This altitude h_{lim} corresponds to the height where there is no more overlap between two references stars at opposite *FoV* limit positions. It is not possible, using wave-front measurements from those two reference stars, to sense a turbulent layer at altitude h_{lim}. This implies that in adaptive systems with DMs conjugated at altitudes separated less than the distance $2h_{\mathrm{lim}}$ all the possible layers are corrected (at least the low frequencies).

2.4.1. GLAO systems

For example, up to 8 m diameter, for a 4 arcmin FoV, $h_{\mathrm{lim}} < 7$ km, much less than the maximum altitude of several turbulent layers (according to the model this altitude is around $H_{\mathrm{max}} = 15$ km). Then, for a GLAO system, high altitude layers (> 7 km) are unseen and uncorrected. This implies that, while the ground layer is corrected, the high layers are not corrected at all, and on the corrected PSF they work, generating a small seeing disk of the order of $\lambda/r_0^{\mathrm{high}}$ (r_0^{high} is the coherence length of the high turbulence). Over 20 m diameters the $h_{\mathrm{lim}} > H$ and also higher layers are low order corrected: on extra-large telescopes all layers are seen by the sensor and corrected by the DM, even if with decreasing accuracy for high ones. In these cases the PSF is composed by the diffraction limited spot over a depressed halo-seeing disk. GLAO for ELT moves the energy in the central peak directly without an efficient high-seeing reduction, or energy concentration. GLAO benefits from ground removal: the seeing disk induced by the higher layer is the dominating part of the remaining turbulence, which gives the PSF shape. The diffraction-limited spike is still present and unavoidable. Increasing the correction by using a smaller sub-aperture for the pupil sampling, or using smaller technical FoV, increases the SR while the halo seeing is depressed. In open loop (case without any AO) also small outer-scales behave a correction, moving the energy from the seeing halo disk to the diffraction peak.

On Fig. 8 is represented a total PSF for a GLAO system on a 10 m class telescope (red) and on a 100 m telescope (black). Both PSF have been computed considering Kolmogorov turbulence, with two layers, the first one at 0 km with $r_0^{\mathrm{low}} = 1$ m and a second one at 20 km with a local $r_0^{\mathrm{high}} = 1.7$ m. We considered a FoV of 6 arcmin assuming a homogeneous distribution of reference stars, which means that we do not simulate the behaviour of a particular kind of wavefront sensor but only the effect due to the smoothing of the not conjugated layers. In other words, we are assuming an ideal WFS without any noise and not reference limited. The ground layer has been corrected, subtracting all the spatial frequencies that could be corrected because seen by the telescope (diffraction limit), while for the high layer correction we took into account the distance from the conjugated plane and the FoV by smoothing the spatial frequencies in the same way an ideal system would.

The spike at the top of the 100 m PSF corresponds to the diffraction-limited core of the partial correction of whole atmosphere and below it the ‘seeing’ halo due mainly to the uncorrected high altitude layers. The behavior of the 10 m telescope correction follows the 100 m down to spatial distances from the center of the PSF of the order of $\lambda/r_{0,\mathrm{high}}$, then the two PSFs diverge: the 10 m shows a ‘plateau’ while the 100 m PSF presents over this the diffraction limited core. In a PSF the dimension of the disk depends strongly on the power in the high spatial frequencies. In 10 m GLAO correction the high layers are not corrected at all, introducing in the WF of the stars seen by the telescope the phase disturbance given by them. In the 100 m case, the low frequencies of the high layers are corrected by the GLAO system and the resulting PSF is composed of a diffraction spike due to the partial correction and to a ‘seeing disk’ halo due to the high order unseen modes.

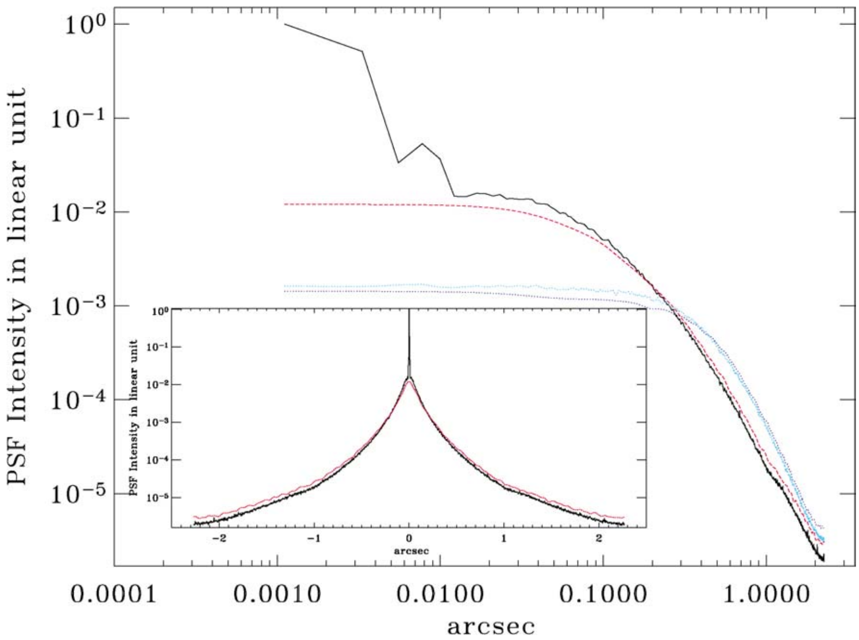

Fig. 8. Comparison of simulated PSF for 10 m (in red) and 100 m case (in black) with axes in log scales, the dotted lines represent the seeing disk intensity profile for the two cases. In the insert the linear unit has been left.

2.4.2. MCAO systems

Since it requires several mirrors to correct efficiently all altitude layers in both cases (10 m or 100 m telescope), the problem presented for the GLAO case, linked to the partial-correction of higher layers, is not present in MCAO, and such system performances can be scaled directly from 8 m existing systems.

3. Conclusion

We presented in this article an analysis of a few key points that represent limitations or constraints in the realization of an MCAO system for an ELT. From the mirror realization to the use of a laser guide star, we have pointed out a few issues that should be solved by further developments and studies. Moreover, we have discussed the behaviour of the corrections on going to such a size, showing that, even from a geometrical point of view, the 10 m class AO differs from the ELT case, underlying how the PSF behaves in the two cases and in the case of a Ground Layer AO or a Multiconjugate AO. Finally, we have showed that some arguments exist, for example the finite outer-scale or the large overlap of the pupil, to say that making an AO for an ELT should be reasonably feasible.

References

[1] G. Rousset, P.-Y. Madec, J.-L. Beuzit, J.-G. Cuby, P. Gigan, P. Léna, F. Rigaut, C. Boyer, J.-P. Gaffard, J.-C. Richard, M. Vittot, E. Gendron, N. Hubin, F. Merkle, The COME-ON-PLUS Project: An adaptive optics system for a 4 meter class telescope, in: Progress in Telescope and Instrumentation Technologies, ESO Conference and Workshop Proceedings, ESO Conference on Progress in Telescope and Instrumentation Technologies, 1992, p. 403.

[2] R. Ragazzoni, A. Baruffolo, J. Farinato, A. Ghedina, E. Marchetti, S. Esposito, L. Fini, P. Ranfagni, F. Bortoletto, M. D'Alessandro, M. Ghigo, G. Crimi, Final commissioning phase of the AdOpt@TNG module, in: P. Wizinowich (Ed.), Adaptive Optical Systems Technology, vol. 4007, 2000, pp. 57–62.

[3] G. Rousset, F. Lacombe, P. Puget, E. Gendron, N. Hubin, G. Zins, E. Stadler, J. Charton, P. Gigan, P. Feautrier, Status of the VLT Nasmyth adaptive optics system (NAOS), in: P.L. Wizinowich (Ed.), Adaptive Optical Systems Technology, in: Proc. SPIE, vol. 4007, 2000, pp. 72–81.

[4] J. Beckers, Increasing the size of the isoplanatic patch with multiconjugate adaptive optics, in: M.-H. Ulrich (Ed.), Very Large Telescopes and Instrumentation, vol. 2, 1988, pp. 693–703.

[5] B.L. Ellerbroek, First-order performance evaluation of adaptive-optics systems for atmospheric-turbulence compensation in extended-field-of-view astronomical telescopes, J. Opt. Soc. Am. A 11 (2) (1994) 783–805.

[6] R. Ragazzoni, E. Marchetti, F. Rigaut, Modal tomography for adaptive optics, Astron. Astrophys. 342 (1999) 53–56.

[7] E. Marchetti, MAD: practical implementation of MCAO concepts, C. R. Physique 6 (2005), this issue.

[8] W. Gaessler, LINC-NIRVANA: MCAO toward Extremely Large Telescopes, C. R. Physique 6 (2005), this issue.

[9] M. Langlois, G. Moretto, K. Richards, S. Hegwer, T.R. Rimmele, Solar multiconjugate adaptive optics at the Dunn Solar Telescope: preliminary results, in: D. Bonaccini, B.L. Ellerbroek, R. Ragazzoni (Eds.), Advancements in Adaptive Optics, in: Proc. SPIE, vol. 5490, 2004, pp. 59–66.

[10] B.L. Ellerbroek, F.J. Rigaut, B.J. Bauman, C. Boyer, S.L. Browne, R.A. Buchroeder, J.W. Catone, P. Clark, C. d'Orgeville, D.T. Gavel, G. Herriot, M.R. Hunten, E. James, E.J. Kibblewhite, I.T. McKinnie, J.T. Murray, D. Rabaud, L.K. Saddlemyer, J. Sebag, J. Stillburn, J.M. Telle, J.-P. Veran, Multiconjugate adaptive optics for Gemini-South, in: P.L. Wizinowich, D. Bonaccini (Eds.), Adaptive Optical System Technologies II, in: Proc. SPIE, vol. 4839, 2003, pp. 55–66.

[11] E. Marchetti, R. Brast, B. Delabre, R. Donaldson, E. Fedrigo, C. Frank, N.N. Hubin, J. Kolb, M. Le Louarn, J.-L. Lizon, S. Oberti, R. Reiss, J. Santos, S. Tordo, R. Ragazzoni, C. Arcidiacono, A. Baruffolo, E. Diolaiti, J. Farinato, E. Vernet-Viard, MAD status report, in: D.B. Calia, B.L. Ellerbroek, R. Ragazzoni (Eds.), Advancements in Adaptive Optics, in: Proc. SPIE, vol. 5490, 2004, pp. 236–247.

[12] R. Soci, R. Ragazzoni, T.M. Herbst, J. Farinato, W. Gaessler, H. Baumeister, R.-R. Rohloff, E. Diolaiti, W.-L. Xu, D.R. Andersen, S.E. Egner, C. Arcidiacono, M. Lombini, M. Ebert, A. Boehm, N. Muench, M. Xompero, LINC-NIRVANA: mechanical challenges of the MCAO wavefront sensor, in: D.B. Calia, B.L. Ellerbroek, R. Ragazzoni (Eds.), Advancements in Adaptive Optics, in: Proc. SPIE, vol. 5490, 2004, pp. 1286–1295.

[13] R. Ragazzoni, J. Farinato, E. Marchetti, Adaptive optics for 100-m-class telescopes: new challenges require new solutions, in: P.L. Wizinowich (Ed.), Adaptive Optical Systems Technology, in: Proc. SPIE, vol. 4007, 2000, pp. 1076–1087.

[14] F. Rigaut, Applied LGS MCAO, C. R. Physique 6 (2005), this issue.

[15] R. Conan, J. Borgnino, A. Ziad, F. Martin, Analytical solution for the covariance and for the decorrelation time of the angle of arrival of a wave front corrugated by atmospheric turbulence, J. Opt. Soc. Am. A: Opt. Image Sci. Vision 17 (10) (2000) 1807–1818.

[16] F.J. Rigaut, B.L. Ellerbroek, R. Flicker, Principles, limitations, and performance of multiconjugate adaptive optics, in: P.L. Wizinowich (Ed.), Adaptive Optical Systems Technology, in: Proc. SPIE, vol. 4007, 2000, pp. 1022–1031.

[17] A. Riccardi, G. Brusa, M. Xompero, D. Zanotti, C. Del Vecchio, P. Salinari, P. Ranfagni, D. Gallieni, R. Biasi, M. Andrighettoni, S. Miller, P. Mantegazza, The adaptive secondary mirrors for the Large Binocular Telescope: a progress report, in: D.B. Calia, B.L. Ellerbroek, R. Ragazzoni (Eds.), Advancements in Adaptive Optics, in: Proc. SPIE, vol. 5490, 2004, pp. 1564–1571.

[18] F. Zamkotsian, H. Camon, N. Fabre, V. Conedera, G. Moreaux, Microdeformable mirror for next-generation adaptive optical systems, in: P.L. Wizinowich, D. Bonaccini (Eds.), Adaptive Optical System Technologies II, in: Proc. SPIE, vol. 4839, 2003, pp. 711–720.

[19] P. Dierickx, J. Beletic, B. Delabre, M. Ferrari, R. Gilmozzi, N. Hubin, The optics of the OWL 100-m adaptive telescope, in: T. Andersen, A. Ardeberg, R. Gilmozzi (Eds.), Proceedings of the Backaskog Workshop on Extremely Large Telescopes, ESO Conference and Workshop Proceedings, vol. 57, 2000, p. 97.

[20] S. Kellner, R. Ragazzoni, W. Gassler, E. Diolaiti, T.J. Morris, C.D. Saunter, R. Meyers, J. Farinato, C. Arcidiacono, A. Ghedina, PIGS: first results on sky, in: D. Bonaccini, B.L. Ellerbroek, R. Ragazzoni (Eds.), Advancements in Adaptive Optics, in: Proc. SPIE, vol. 5490, 2004, pp. 989–997.

[21] T. Butterley, D.F. Buscher, G.D. Love, T.J. Morris, R.M. Myers, R.W. Wilson, Sky-projected Shack–Hartmann laser guide star, in: D.B. Calia, B.L. Ellerbroek, R. Ragazzoni (Eds.), Advancements in Adaptive Optics, in: Proc. SPIE, vol. 5490, 2004, pp. 966–973.